ISSN 0024-4902, Lithology and Mineral Resources, 2018, Vol. 53, No. 2, pp. 110–129. © Pleiades Publishing, Inc., 2018.
Original Russian Text © A.V. Maslov, V.P. Shevchenko, V.A. Bobrov, E.V. Belogub, V.B. Ershova, O.S. Vereshchagin, P.V. Khvorov, 2018, published in Litologiya i Poleznye Iskopaemye, 2018, No. 2, pp. 121–141.

Mineralogical–Geochemical Features of Ice-Rafted Sediments in Some Arctic Regions

A. V. Maslov[a], *, V. P. Shevchenko[b], **, V. A. Bobrov[c], *, E. V. Belogub[d], ****, V. B. Ershova[e], *****, O. S. Vereshchagin[e], and P. V. Khvorov[d]**

[a]*Zavaritskii Institute of Geology and Geochemistry, Ural Branch, Russian Academy of Sciences, ul. Vonsovskogo 15, Yekaterinburg, 620016, Russia*

[b]*Shirshov Institute of Oceanology, Russian Academy of Sciences, Nakhimovskii pr. 36, Moscow, 117997 Russia*

[c]*Sobolev Institute of Geology and Mineralogy, Siberian Branch, Russian Academy of Sciences, pr. akad. Koptyuga 3, Novosibirsk, 630090 Russia*

[d]*Institute of Mineralogy, Ural Branch, Russian Academy of Sciences, Ilmeny Reserve, Miass, Chelyabinsk obl., 456317 Russia*

[e]*Institute of Earth Sciences, St. Petersburg State University, Universitetskaya nab. 7/9, St. Petersburg, 199034 Russia*

**e-mail: amas2004@mail.ru*

***e-mail: vshevch@ocean.ru*

****e-mail: bobr@igm.nsc.ru*

*****e-mail: belogub@mineralogy.ru*

******e-mail: v.ershova@spbu.ru, o.vereshchagin@spbu.ru*

Received October 29, 2016

Abstract—The quantitative mineral composition estimated using the Rietveld method and some geochemical features are considered for bulk samples of the ice-rafted sediments (IRS) from some Arctic regions. Layer silicates in the studied samples vary from ~20 to ~50%. They are dominated by micas and their decomposition products (illite and likely some part of smectites) at significant contents of kaolinite, chlorite, and transformation/decomposition products of the latter. A significant content of illite and muscovite among layer silicates in most IRS samples suggests that sources of the sedimentary material were mainly mineralogically similar to modern bottom sediments of the East Siberian and Chukchi seas, as well as presumably sediments of the eastern Laptev Sea. It is suggested that a significant kaolinite fraction in IRS samples from the North Pole area can be caused by the influx of ice-rafted fine-grained sedimentary material from the Beaufort or Chukchi seas, where kaolinite is supplied from the Bering Sea. Positions of IRS data points in the $(La/Yb)_N$–Eu/Eu*, $(La/Yb)_N$–$(Eu/Sm)_N$, and $(La/Yb)_N$–Th diagrams show that the studied samples contain variable proportions of erosion products of both mafic and felsic magmatic rocks and/or sufficiently mature sedimentary rocks. This conclusion is confirmed by localization of IRS data points in the Th/Co–La, Si/Al–Ce, and Si/Al–Sr diagrams.

DOI: 10.1134/S0024490218020037

INTRODUCTION

The Arctic Sea ice not only accumulates significant amounts of the dissolved and suspended particulate matters, but also plays an important role in their transportation and redeposition (Herman, 1989; Kassens and Thiede, 1994; Lisitzin, 1994, 2010; Lisitzin and Shevchenko, 2016; Nürnberg et al., 1994; Pfirman et al., 1990, 1995; and others). Ice rafting of sediments and their discharge at the warm water boundary to the south of Fram Strait and in the Kuroshio–Oyashio current collision region contribute significantly to the formation of the unique sedimentary depocenters (Dethleff and Kuhlmann, 2010; Eicken et al., 1997 Levitan et al., 2007; Lisitzin, 1994, 2010; Nürnberg et al., 1994; Pfirman et al., 1990, 1995; Wollenburg, 1993].

Solid matter is incorporated in sea ice due to the trapping of suspended particulates from water sequence by sludge ice and bottom or intrawater ice. This is especially efficient for the silt- and pelite-sized particles. Definite part of ice-rafted sediments (IRS) also is of eolian nature and supplied with wind from Arctic islands and coast (Lisitzin, 1994, 2010; Shevchenko et al., 2002). The mineralogical and geochemical study of fine-grained sediments together with the petrographic data on rock fragments and species composition of macro- and microfossils makes it possible to reconstruct the direction of transport of ice-rafted sediments and their possible sources.

The main trajectory of ice flows, the Transpolar Drift, passes through the Arctic Ocean from the Chukchi and East Siberian seas to the Fram Strait. The most important "ice factories" in the Arctic region are the Laptev Sea and, partly, the East Siberian Sea (Lisitzin, 2002, 2010; Zakharov, 1996). Up to a few hundred grams of sedimentary material is incorporated in ice during the formation of 1 m^3 ice in a shallow-water region of the Laptev Sea (Dethleff et al., 1993; Reimnitz et al., 1994). Less favorable conditions for the mobilization of sedimentary material occur in the Beaufort Sea, which has much narrower shelf and usually is covered by ice during summer (Eicken et al., 1997; Kolatschek et al., 1996; Pfirman et al., 1990; Reimnitz et al., 1994).

A complex approach is required to determine the exact position of provenance of ice-rafted sediments in each certain case. This is caused, on the one hand, by complex ice circulation in the Arctic Basin, and, on the other hand, by paucity of data on the IRS composition. According to many researchers, the main IRS suppliers are the wide shallow-water shelves of some Arctic seas (Colony et al., 1991; Darby et al., 2011; Lisitzin, 2002; Lisitzin and Shevchenko, 2016; Nürnberg et al., 1994; and others).

Several methods are used to establish sources and IRS transport pathways in the Arctic region (Andrews and Eberl, 2007, 2012; Andrews and Hardardottir, 2009; Darby et al., 1989; Farmer et al., 2006; Grousset et al., 2001; Hemming et al., 2002; Lisitzin, 1994, 2010; Moros et al., 2004; Nürnberg et al., 1995; Pirrung et al., 2002; Verplanck et al., 2009; Wollenburg, 1993): (1) mineralogical study of sand, clay, and heavy fractions; (2) analysis of radiogenic isotopes; (3) Ar-Ar dating; (4) study of magnetometric characteristics and others. This work reports the results of following studies: (1) X-ray study of the bulk composition of IRS samples, as well as the composition of clay fraction (<1 μm) performed selectively for some samples (because of a small amount of available material); (2) analysis of some lithogeochemical features providing insight into possible IRS sources in ices of the central and western Arctic region.

MATERIALS AND METHODS

The studied sedimentary material dispersed in ice was collected during Cruise ARK-XIV/1a of the R/V *Polarstern* in 1998 in the central Arctic region (*Arctic '98 ...,* 1999), as well as during Cruise ARK-XX/3 of the R/V *Polarstern* in 2004, in the Yermak Plateau area and Fram Strait (*Scientific ...*, 2005). The sediments occur as cryoconite pellets 1–10 mm long distributed in the top 1–2 cm ice layer, where snow thawed on the ice surface. Samples were collected with a stainless steel knife and a plastic scoop into plastic jars.

The collected material characterizes IRS from four regions, which further are termed as follows: A (area between the New Siberian Islands and North Pole), B (North Pole area), C (north of Spitsbergen) and D (Yermak Plateau area, Western Arctic region) (Fig. 1).

The X-ray phase analysis of powdered IRS samples from the Yermak Plateau area was carried out at the Resource Center of the St. Petersburg State University "X-ray Diffraction Methods of Study" on a Rigaku Miniflex II diffractometer (Co-Kα radiation, record interval (2θ) within 3°–60°, record rate of 2°/min, and a step of 0.02°). The obtained X-ray powder diffraction patterns were processed using a PDXL II software package. Phases were identified using the ICDD (PDF-2/Release 2011 RDB) data base (DB). Clay minerals were analyzed in detail in fractions obtained by the decantation in water with the subsequent centrifuging. Oriented specimens were prepared by the precipitation from suspension on mounts. Suspended fractions with particle size of <10, <1, and <0.1 μm were collected using standard procedures. Qualitative analysis of clay minerals was carried out in <1 μm fraction oriented specimens of air-dried, glycolated, and heated (for 4 h at 550°C) samples.

The IRS samples collected during Cruise XIV/1a were analyzed on a SHIMADZU XRD-6000 X-ray diffractometer (Cu-Kα monochromatic radiation, record rate of 2°/min for bulk samples and 1°/min for the clay fraction) at the Institute of Mineralogy of the Ural Branch of the Russian Academy of Sciences. The X-ray diffraction patterns were obtained for maximally disoriented powdered specimens of bulk samples. The quantitative composition of the samples was determined by the Rietveld method (SIROQUANT V.3 software package). Internal DB of the software package (quartz, albite, maximum microcline, orthoclase, actinolite, edenite, muscovite, kaolinite, and montmorillonite) and, additionally, own data on clinochlore, Fe-rich dolomite, and illite were used as reference samples. The calculations also involved the possible texturing of the studied specimens and disordering of the crystalline structure of layer silicates, which leads to an increase of the reflection half-width. Maximum mathematical error seemed to be related to estimation of the muscovite content. The clay fraction was extracted from sample IRS-1 by decantation for 12 h and subsequent centrifuging. Oriented specimen was obtained by precipitation in alcohol. The specimen was analyzed in the air-dried, glycerin intercalation, and heated (at 550°C for 1 h) state using standard technique (*Rentgenografiya ...*, 1983].

The Si and Al contents were determined by the photometric method (Gelman and Starobina, 1976) at the Institute of Oceanology of the Russian Academy of Sciences (analyst A.B. Isaeva). Contents of rare and trace elements in IRS samples collected during Cruise ARK-XIV/1a were analyzed by two different methods. The instrumental neutron-activation analysis (INAA)

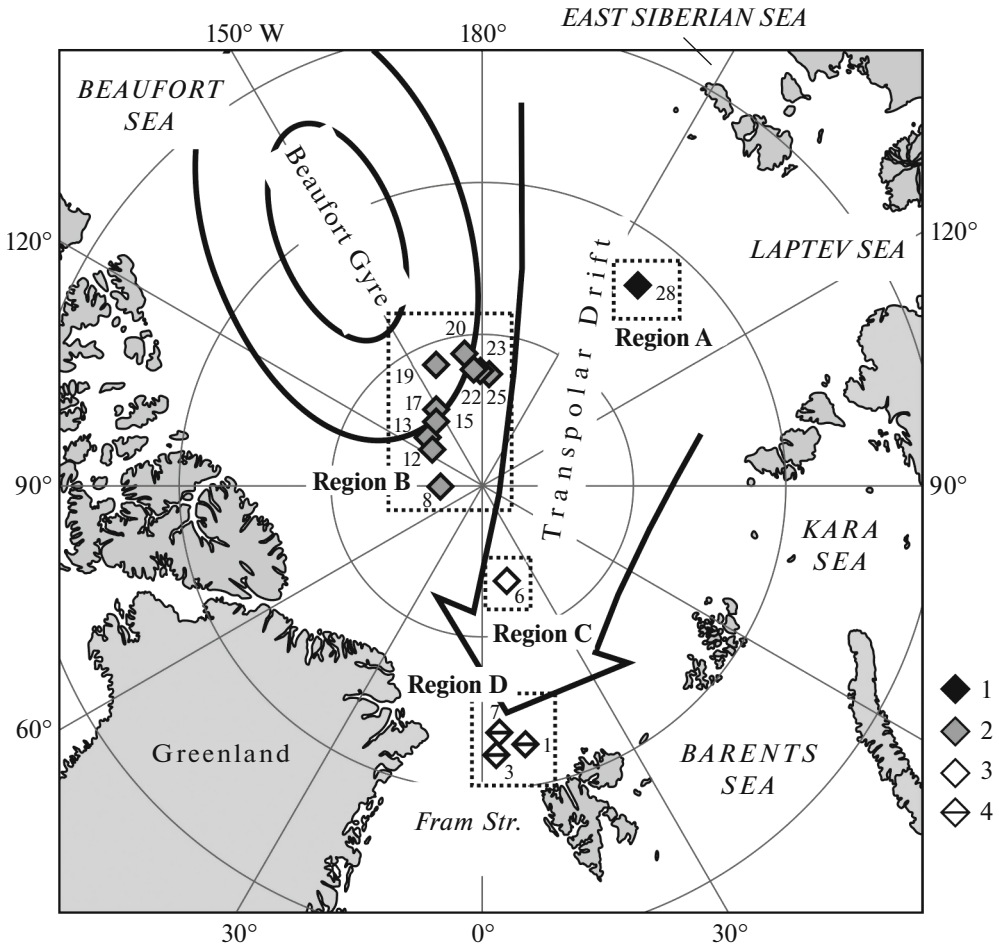

Fig. 1. Position of the studied IRS samples collected during cruises ARK-XIV/1a (1998) and ARK-XX/3 (2004) of the R/V *Polarstern*. (1) Samples from region A; (2) samples from region B; (3) sample from region C; (4) sample from region D.

was carried out using technique (Bobrov et al., 2001, 2001a) after sample radiation in an active zone of nuclear reactor of the Tomsk Polytechnical Institute by a thermal neutron flux (2.8×10^{13} neutron/cm^2/s) for 5 h. Spectrometric analysis was carried out using the planar HPG and coaxial detectors Ge/(Li) analyzed within the range of 30–2000 keV. In this range, we determined gamma-radiation and characteristic radiation of radionuclides with the half-decay life of days, months, and years. Each sample was analyzed for La, Ce, Nd, Sm, Eu, Gd, Tb, Yb and Lu contents. The second method, ICP-MS, was conducted at the Institute of Geology and Geochemistry of the Ural Branch of the Russian Academy of Sciences using technique (Votyakov et al., 2006), as well as at the Institute of Mineralogy of the Ural Branch of the Russian Academy of Sciences (analyst K.A. Filippova). The trace-element contents in IRS samples from the Yermak Plateau area were determined by ICP-MS at the Institute of Geology and Geochemistry of the Ural Branch of the Russian Academy of Sciences (analysts D.V. Kiseleva, N.N. Adamovich, N.V. Cherednichenko, O.A. Berezikova, and L.K. Deryugina).

RESULTS OF THE X-RAY PHASE STUDY OF IRS SAMPLES

According to microscopic studies of smear slides, IRS samples are mainly made up of the silt–pelite fraction. The pelite fraction accounts for 30 to 70% (on average, 45–50%) (Shevchenko et al., 2016). The silt fraction has a quartz–feldspathic composition dominated by feldspars, with the following widespread minerals (in order of decreasing content): micas (muscovite, biotite), chlorite, amphiboles (hornblende, actinolite–tremolite series), and pyroxenes (aegirine–augite, hypersthene, hedenbergite). Accessory minerals are zircon and disthene. The amount of biogenic component in IRS on average is 5–10%. It is mainly represented by diatom algae, as well as by radiolarians and sponge spicules.

According to the X-ray phase analysis, IRS samples are mainly made up of terrigenous minerals:

Table 1. Results of quantitative assessment of the mineral composition of IRS samples from regions A, B, C, and D using the Rietveld method (SIROQUANT V.3), wt %

Region	Sample no.	Quartz	Albite	KFsp*	Amphibole	Carbonate**	Total layer silicates	Fraction among layer silicates		
								Illite*** + muscovite	Chlorite****	Kaolinite
A	XIV/1a-28	34.0	12.4	4.0	–		49.5	60	9	31
B	XIV/1a-8	36.6	28.6	14.7	tr.		19.9	69	15	16
	XIV/1a-12	37.8	23.6	6.0	1.2		31.4	74	10	17
	XIV/1a-13	32.9	18.9	6.0	0.7	tr.	41.5	63	12	26
	XIV/1a-15	41.9	25.3	12.4	1.8		18.5	62	15	23
	XIV/1a-17	29.6	18.2	8.1	–		43.9	45	16	39
	XIV/1a-19	32.6	19.7	5.3	0.5	tr.	41.8	63	11	27
	XIV/1a-20	27.7	18.0	4.9	tr.		48.9	64	15	22
	XIV/1a-22	38.2	23.6	4.7	1		32.6	67	10	22
	XIV/1a-23	36.7	24.7	6.2	–		32.4	64	20	16
	XIV/1a-25	28.1	20.6	7.1	tr.		44.1	61	14	25
C	XIV/1a-6	28.2	25.1	7.0	tr.	tr.	36.5	68	10	22
D	IRS-1	29.5	17.7	7.3	1.1	tr.	44.5	59	11	30

(*) Microcline and orthoclase; (**) mainly dolomite; (***) including unhydrated (true) micas; (tr.) content < 0.5 wt %; (****) in the group of chlorite in this case admixtures of smectite are included. Dash—not detected.

quartz, feldspars (sodic plagioclase, microcline, orthoclase), amphiboles (tremolite–actinolite series, hornblende), micas, and Fe–Mg-chlorite. Some samples contain trace carbonates. Layer silicates are highly hydrated, which follows from an increase of the half-width value and asymmetrical first basal reflections. Clay minerals are dominated by illite, chlorite/disordered mixed-layer chlorite–smectite, smectite, and kaolinite. It should be noted that X-ray patterns show slightly elevated background, which indicates the presence of X-ray amorphous phase (Table 1, Fig. 2).

As seen in Table 1, sample XIV/1a-28 collected in region A contains 60% illite and muscovite, while the content of chlorite is approximately three times lower than that of kaolinite (9 and 31%, respectively). The IRS samples collected in the North Pole area (region B) can be relatively arbitrarily ascribed to three groups/assemblages of layer silicates. The first group (samples XIV/1a-8, XIV/1a-13, XIV/1a-15, XIV/1a-19, XIV/1a-20, XIV/1a-22, XIV/1a-23, and XIV/1a-25) contains 61 to 69% illite and muscovite, while the chlorite content varies from 10 to 20%. In terms of the composition of layer silicates, samples of this group are close to sample XIV/1a-6 collected in region C (Fig. 1). The second group (sample XIV/1a-12) contains up to 74% illite and muscovite, while chlorite and kaolinite account for 10% and 17%, respectively. Sample XIV/1a-17 with illite plus muscovite decreasing to 45% and kaolinite increasing to 39% is ascribed to the third group.

Samples IRS-1, IRS-3, and IRS-7 collected in the Yermak Plateau area (region D) were analyzed in more detail. The clay fraction (<1 μm) of all aforementioned samples, as compared to other samples, shows a sharp increase in the X-ray amorphous component, which follows from an increase in background, half-width value, and complicated shape of reflections of layer silicates (Figs. 3, 4). The latters, judging from the above-mentioned features, contain smectite layers.

According to data obtained at the Institute of Mineralogy of the Ural Branch of the Russian Academy of Sciences, the clay fraction (<1 μm) of sample IRS-1 contains a significant amount of smectitized chlorites and kaolinite against the background of the general illite predominance. The presence of smectite layers in the chlorite structure indicates the peculiar behavior of glycerin-saturated and heated specimens. After glycerin saturation, the basal reflections ~14 Å ($2\Theta_{Cu}$ ~6.2–6.3°, chlorite and smectite) and ~10 Å ($2\Theta_{Cu}$ ~8.8–8.9°, micas, illite) become wider, and show decrease in their intensity and increase of low-angle background. After heating, the first and third basal reflections of chlorite at ~14 and ~3.54–3.56 Å ($2\Theta_{Cu}$ ~25.15–25.02°) were recovered. However, the effect of doubling of the latter due to the kaolinite interference disappears, while the reflection of mica (illite) at ~10 Å is preserved (Fig. 3). The above-mentioned features indicate a significant transformation of micas and chlorite, disordered arrangement of smectite layers in them, and kaolinite presence.

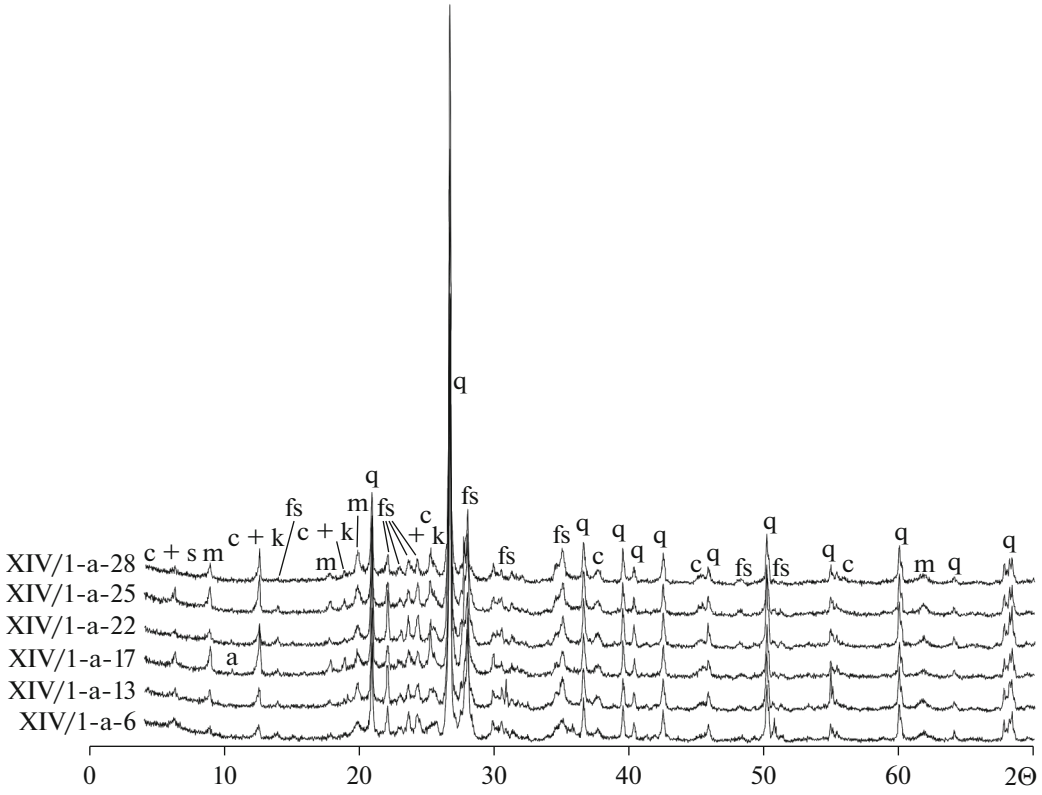

Fig. 2. X-ray diffraction patterns of samples IRS XIV/1a-28, -13, -17, -22, -25, and -6, taken in the regions A, B, and C (Fig. 1). (c) Chlorite; (s) smectite; (m) mica; (k) kaolinite; (fs) feldspars; (q) quartz; (a) amphibole.

According to the X-ray phase analysis performed at the St. Petersburg State University, the clay fraction of samples IRS-3 and IRS-7 contains smectite, chlorite, illite, and kaolinite. Ethylene glycol-saturated samples show the well-expressed smectite reflection with center at ~17 Å ($2\Theta_{Cu}$ ~ 5.2°). Heating resulted in the recovery of reflection series corresponding to chlorite and mica (Fig. 4). In spite of the fact that X-ray studies at the Institute of Mineralogy of the Ural Branch of the Russian Academy of Sciences and at the St. Petersburg State University were carried out using different diffractometers, reagents for saturation, and heating time, the obtained results are quite comparable.

To sum up, the following conclusions can be drawn. The quartz content in IRS samples varies from 29% (region C) to 42% (region B), and albite varies from 12% (region A) to 25% (regions B and C). The maximum K-Fsp content reaches ~15% (sample XIV/1a-8, region B), while the lowest content is 4% (region A). The total content of clay minerals varies from 37% (region C) to 49–50% (regions A and B). The content of illite and muscovite in IRS samples from regions A and D is around 60%, slightly higher (68%) in the IRS from region C, and varies from 45% to 74% in samples from region B. The chlorite contents in IRS samples from regions A, C, and D are comparable (9–10%) and may reach 15 to 16% or even 20% of the total content of clay minerals in some samples from region B. At last, the minimum (16%) and maximum (39%) contents of kaolinite were found in IRS samples from region B. Comparable content of kaolinite (~30%) was determined in samples from regions A and D, while sample XIV/1a-6 (region C) contains around 22% kaolinite. This is the general characteristics of studied samples, detail of which will be described and analyzed below.

RESULTS OF THE GEOCHEMICAL STUDY OF IRS SAMPLES

It is required to compare rare and trace elements data on IRS samples obtained by the INAA (Table 2) and ICP-MS (Table 3) methods to test the consistency of the data[1]. Figure 5 shows the contents of Sc, Cr, Co, Zn, Rb, Zr, Cs, Ba, La, Ce, Nd, Sm, Eu, Tb, Yb, Lu, Hf, and Th determined by both methods in IRS sam-

[1] It was made to avoid confusion related to the application of different methods (INAA and ICP-MS) with different uncertainties, which may affect the distribution of data points in different diagrams. Of great importance in this aspect is that the great body of analytical data on composition of bottom sediments of the Arctic Ocean and other oceans and seas were obtained by the end of the 20th century by the INAA method. In this relation, it is very important to understand how these data can be used together with ICP-MS data.

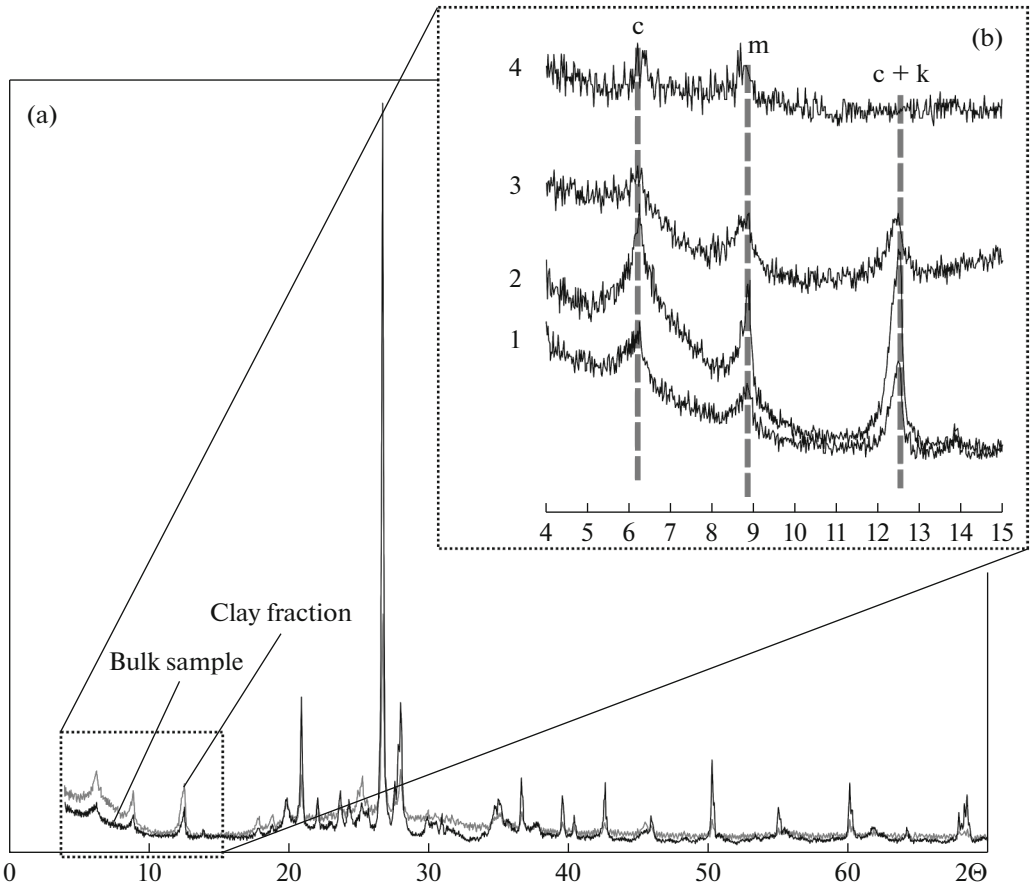

Fig. 3. X-ray powder diffraction pattern of IRS-1 bulk sample collected in the Yermak Plateau area (a) and oriented specimens of clay fraction (<1 μm), extracted from this sample (b). (1) Bulk sample; (2–4) clay fraction: (2) air-dried, (3) glycerin-saturated, (4) heated at 550°C. Other symbols are shown in Fig. 2.

ples taken during Cruise ARK-XIV/1a, as well as average ratios of the aforementioned elements (ICP-MS/INAA). Their comparison showed that the elements can be divided into several groups: (1) Ba with the average content (C) determined by INAA equal to $1.20 \times C_{ICP\text{-}MS}$; (2) trace elements (Sc, Cr, Co, Zn, Rb, Cs, Sm, Eu, and Th) with the ICP-MS-determined content varying from 0.85 to $1.15 \times C_{INAA}$ (i.e., they are comparable); (3) La, Ce, Nd, Tb, Yb, and Lu with the ICP-MS-determined content varying from 0.50 to $0.85 \times C_{INAA}$; and (4) Zr and Hf with the $C_{average}$ content determined by ICP-MS reaching no more than half of the INAA-determined concentrations.

Some differences in contents of the above-mentioned elements established by two different methods further served as the basis for separate (INAA and ICP-MS data sets) analysis of binary diagrams, comparison of the trace element composition of IRS samples and modern bottom sediments from the large Arctic rivers. The PAAS-normalized rare and trace element contents in IRS samples from regions A, B, and C determined by the ICP-MS method show that the concentrations of most elements in the majority of samples are below those of the average post-Archean Australian Shale (PAAS) (Taylor and McLennan, 1985) (Fig. 6), while samples from different regions show some differences. However, more representative data sets are required to estimate the statistic significance of these differences. In particular, only Cu and Ba contents in sample XIV/1a-28 (region A) are similar to those of PAAS[2]. The Co, Sr, Y, Zr, Nb, Mo, Sn, Cs, La, Ce, Ho, Er, Tm, Yb, Lu, Hf, and Th contents are < 0.50 × PAAS. The average concentrations of Zn, Ba, Sm, Eu, Gd, and Pb in the ice-rafted sediments from region B (samples XIV/1a-8, XIV/1a-12, XIV/1a-13, XIV/1a-15, XIV/1a-17, XIV/1a-19, XIV/1a-20, XIV/1a-22, XIV/1a-23, XIV/1a-25) are comparable with those of PAAS. The Cu, Zr, Nb, Sn, Cs, and Hf contents here are below 0.50×PAAS. The Zn, Sm, Eu, and Gd contents in IRS sample XIV/1a-6 (region C) are comparable with PAAS contents. The Cu, Zr, Sn, and Cs contents in this sample are less than 0.50 × PAAS, while the Sr content is 1.18 ×

[2] Contents of 0.85–1.15 × PAAS are arbitrarily regarded as comparable with PAAS.

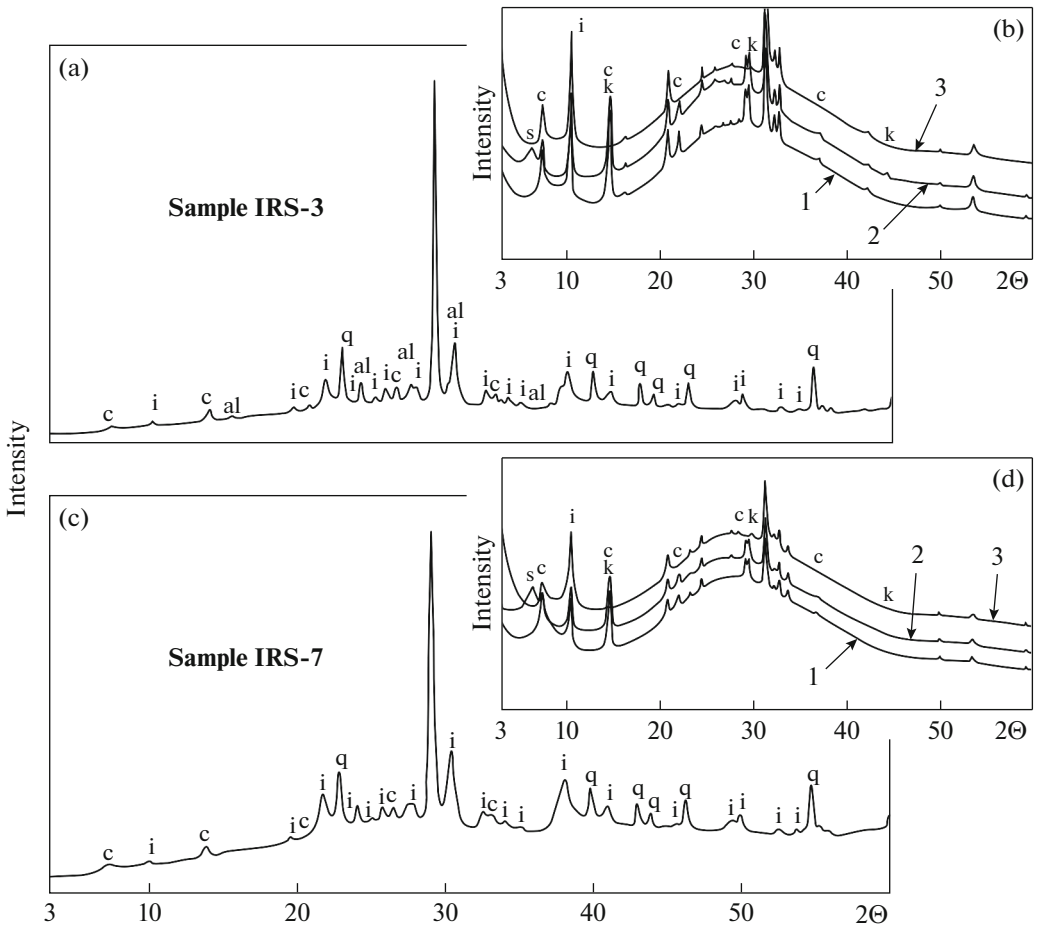

Fig. 4. X-ray diffraction patterns of IRS-3 and IRS-7 bulk samples collected in the Yermak Plateau area (a, c) and oriented specimens of clay fraction (<1 μm) extracted from these samples (b, d): (1) in the air-dried state, (2) glycerin-saturated, (3) heated at 550°C. (i) Illite and muscovite; (al) albite. Other symbols are shown in Fig. 2.

PAAS. Contents of other trace elements account for 0.50–0.85 × PAAS.

Our previous study of the trace element composition of modern bottom sediments from the mouth zones of large Russian and Canadian Arctic rivers showed that the distribution of trace and rare elements in them correlates well with the composition of their water drainage areas. The fine (pelitic and silt-pelitic) material of modern bottom sediments of the mouth zones of the Russian Arctic rivers belong mainly to classes 1 and 2 of bottom sediments of the mouth zones of the world's rivers (large rivers and other rivers, the drainage areas of which are made up mainly of sedimentary rocks with definite contribution of mafic magmatic rocks according to (Bayon et al., 2015) (in our case, Severnaya Dvina and Ob rivers), and, with some assumptions, to class 4 (bottom sediments of rivers draining volcanic rocks (Yenisei, Khatanga, Kheta, and others). Bottom sediments of the Lena River in terms of REE and Th distribution are ascribed to class 3 (rivers draining the metamorphic or igneous terranes (Bayon et al., 2015)). The present-day bottom sediments of the Mackenzie River are ascribed to class 1 (Bayon et al., 2015).

Figure 7 based on materials (Emeis, 1985; Konta, 1985; Gaillardet et al., 1999; Gordeev et al., 2004; Kontorovich, 1968; Lisitzin et al., 1980; Martin and Meybeck, 1979; Morozov et al., 1974; Rachold et al., 1996; Rachold, 1999; Savenko, 2006; Savenko et al., 2004)[3], presents the distribution of data points of IRS compositions from different regions (according to ICP-MS data) and data points of the average composition of modern sediments and suspended particulate matter from the mouth zones of the Arctic Russian and Canadian rivers in the $(La/Yb)_N$–Eu/Eu*, $(La/Yb)_N$–$(Eu/Sm)_N$[4], and $(La/Yb)_N$–Th diagrams. The first of the diagrams proposed in (Taylor and MacLennan, 1985) makes it possible to discriminate

[3] Data from the same publications were used for plotting other diagrams of this work.

[4] Parameter $(Eu/Sm)_N$ is considered as the measure of Eu anomaly (Dubinin, 2006) if the Gd content was not determined, for instance, during the INAA analysis.

Table 2. Contents of some rare and trace elements in IRS samples from different regions of Arctic Ocean determined by the INAA method (ppm)

Component	Regions											
	A	B										C
	IRS samples											
	XIV/1a-28	XIV/1a-8	XIV/1a-12	XIV/1a-13	XIV/1a-15	XIV/1a-17	XIV/1a-19	XIV/1a-20	XIV/1a-22	XIV/1a-23	XIV/1a-25	XIV/1a-6
Sc	13.5	7.8	14. 0	11.0	9.0	11.0	14.8	15. 5	12.8	10.0	14.0	12.0
Cr	85.0	53.0	37.0	63.0	48.0	53.0	61.0	61.0	56.0	51.0	61.0	67.0
Co	17.0	9.0	7.8	13.0	10.5	9.0	15.0	16.0	15.0	12.0	13.0	13.0
Zn	60.0	60.0	82.0	85.0	75.0	100.0	92.0	85.0	88.0	95.0	97.0	60.0
Rb	126.0	74.0	60.0	85.0	69.0	68.0	95.0	97.0	86.0	71.0	100.0	63.0
Sr	–	200.0	130.0	168.0	145.0	135.0	150.0	138.0	–	–	–	185.0
Y	–	24.5	23.0	28.5	22.0	22.0	32.0	33.0	–	–	–	23.0
Zr	–	215.0	160.0	165.0	180.0	165.0	195.0	160.0	–	–	–	190.0
Nb	–	10.0	11.0	12.0	9.5	10.0	13.0	11.2	–	–	–	11.0
Cs	7.3	3.1	6.0	4.9	3.6	4.9	7.3	8.0	3.5	4.5	8.5	4.3
Ba	–	530.0	400.0	480.0	440.0	500.0	520.0	520.0	–	–	–	450.0
La	35.0	24.0	25.0	36.0	28.5	25.0	34.0	34.0	36.0	37.0	32.0	35.0
Ce	63.0	60.5	47.0	70.0	56.0	44.0	70.0	73.0	64.0	65.0	60.0	57.0
Pr	–	6.3	6.0	5.5	5.5	–	–	–	–	–	–	5.2
Nd	38.0	32.0	22.0	32.0	25.0	21.0	39.0	29.0	28.5	26.0	31.0	29.0
Sm	6.8	5.2	4.2	6.2	4.9	4.3	7.0	6.2	6.4	5.9	5.0	5.2
Eu	1.4	1.2	0.9	1.2	1.0	0.9	1.4	1.4	1.4	1.1	1.3	1.3
Tb	1.2	0.8	0.6	0.8	0.7	0.6	0.9	1.9	0.8	0.8	0.9	0.8
Yb	3.3	2.2	1.7	2.2	2.0	2.1	3.2	2.8	3.0	2.7	2.7	2.2
Lu	0.4	0.3	0.2	0.3	0.3	0.3	0.5	0.4	0.4	0.3	0.4	0.3
Hf	5.2	5.2	3.9	4.6	2.9	3.5	4.8	4.2	5.6	4.3	4.7	4.9
Th	9.0	7.3	5.6	8.9	7.3	6.5	9.3	8.8	8.4	8.4	8.8	7.2

Dash means data are absent.

Table 3. Contents of rare and trace elements in IRS samples from different regions of the Arctic Ocean determined by the ICP-MS method (ppm)

Components	Regions														
	A	B										C	D		
	IRS samples														
	XIV/1a-28	XIV/1a-8	XIV/1a-12	XIV/1a-13	XIV/1a-15	XIV/1a-17	XIV/1a-19	XIV/1a-20	XIV/1a-22	XIV/1a-23	XIV/1a-25	XIV/1a-6	IRS-1	IRS-3	IRS-7
Li	37.80	32.60	43.10	45.20	40.40	41.60	60.20	65.00	45.80	43.30	61.80	37.60	35.32	47.38	45.41
Sc	11.10	8.87	12.00	10.90	10.50	12.60	13.60	15.70	11.70	10.50	13.20	11.70	16.50	14.60	13.23
V	121.00	77.60	102.00	101.00	90.10	133.00	123.00	132.00	101.00	93.60	142.00	114.00	160.86	142.82	179.20
Cr	63.00	48.60	62.70	63.70	55.20	69.80	62.40	73.40	53.50	49.90	69.10	70.10	85.70	84.39	93.81
Co	8.81	10.60	14.30	13.80	11.90	9.31	13.90	15.60	13.10	11.40	11.90	15.30	15.86	17.74	19.54
Ni	25.50	27.60	31.50	31.70	26.40	28.00	30.70	35.40	24.60	23.40	28.90	33.50	33.57	37.63	41.32
Cu	50.90	26.70	20.70	29.20	19.30	15.30	36.90	38.00	18.50	16.00	19.90	19.10	23.73	25.61	26.30
Zn	68.70	60.70	77.30	81.70	66.20	90.00	101.00	108.00	74.10	71.00	94.20	74.80	110.09	140.74	151.48
Rb	79.90	84.40	95.10	99.10	95.40	85.30	103.00	114.00	85.90	77.70	107.00	85.50	132.24	139.64	124.36
Sr	91.70	204.00	188.00	166.00	179.00	141.00	144.00	143.00	163.00	159.00	151.00	237.00	144.28	128.36	115.37
Y	11.80	14.70	19.20	17.20	16.60	13.90	17.60	20.00	16.50	15.40	17.10	17.80	16.40	16.00	14.97
Zr	48.80	71.20	84.00	72.10	75.20	59.10	72.50	78.30	72.90	61.20	64.70	88.60	114.47	121.86	127.84
Nb	4.16	7.53	8.89	7.81	8.34	6.08	7.38	8.56	6.91	7.38	6.80	9.42	11.74	13.20	12.78
Mo	0.39	0.47	0.99	0.75	0.65	0.42	0.51	0.92	0.79	0.80	0.46	0.69	1.58	1.50	1.43
Cs	5.62	3.53	4.94	5.27	4.72	5.79	6.83	7.36	5.14	4.40	7.97	3.98	4.84	5.12	5.06
Ba	660.00	593.00	550.00	574.00	572.00	682.00	564.00	558.00	515.00	498.00	615.00	546.00	406.05	380.46	304.81
La	17.90	25.10	29.20	28.90	27.80	20.40	25.80	29.30	24.20	23.40	23.90	28.30	25.04	28.22	26.18
Ce	35.20	50.10	59.40	58.70	55.60	41.10	53.60	59.30	48.40	47.40	48.00	57.20	53.58	57.22	50.93
Pr	4.48	6.07	7.36	6.96	6.78	5.10	6.49	7.64	6.19	6.05	6.09	6.72	6.42	6.82	6.32
Nd	17.30	23.10	27.30	25.80	25.80	19.90	25.40	28.90	23.20	23.60	23.30	26.20	24.54	25.05	23.48
Sm	3.69	4.33	5.66	5.29	4.88	4.03	5.25	6.30	4.85	4.52	4.98	5.02	4.78	4.64	4.42
Eu	0.78	0.97	1.10	1.12	1.01	0.92	1.19	1.26	1.06	1.06	1.04	1.06	1.24	1.11	1.05
Gd	3.00	3.73	4.59	4.33	4.02	3.47	4.45	4.99	4.02	3.90	4.16	4.20	5.01	4.84	4.64
Tb	0.39	0.50	0.62	0.66	0.58	0.47	0.60	0.76	0.57	0.53	0.60	0.58	0.66	0.60	0.57
Dy	2.42	3.02	3.69	3.48	3.11	2.79	3.56	3.87	3.28	2.98	3.37	3.49	3.89	3.46	3.29
Ho	0.43	0.57	0.68	0.65	0.62	0.50	0.66	0.72	0.62	0.58	0.64	0.68	0.77	0.69	0.65
Er	1.14	1.61	1.93	1.82	1.82	1.51	1.95	2.03	1.78	1.62	1.78	1.95	2.22	2.01	1.79
Tm	0.18	0.22	0.27	0.26	0.26	0.21	0.25	0.29	0.25	0.22	0.27	0.26	0.33	0.30	0.26
Yb	1.18	1.51	1.85	1.70	1.68	1.40	1.82	1.81	1.68	1.34	1.77	1.90	2.42	1.89	1.73
Lu	0.18	0.23	0.28	0.23	0.24	0.20	0.26	0.30	0.25	0.21	0.28	0.23	0.33	0.29	0.25
Hf	1.42	2.07	2.56	2.15	2.19	1.95	2.33	2.28	2.25	1.92	1.92	2.74	3.66	3.70	3.81
Pb	15.60	17.20	19.40	19.90	17.90	17.90	22.70	24.70	17.60	16.80	21.70	14.90	17.06	20.13	19.32
Th	6.15	7.16	9.44	8.99	8.44	6.88	7.61	9.14	6.91	6.10	8.23	8.33	7.17	7.36	6.71
U	2.09	1.50	1.73	1.69	1.64	2.41	1.68	2.18	1.56	1.74	1.84	1.75	1.99	2.02	1.93

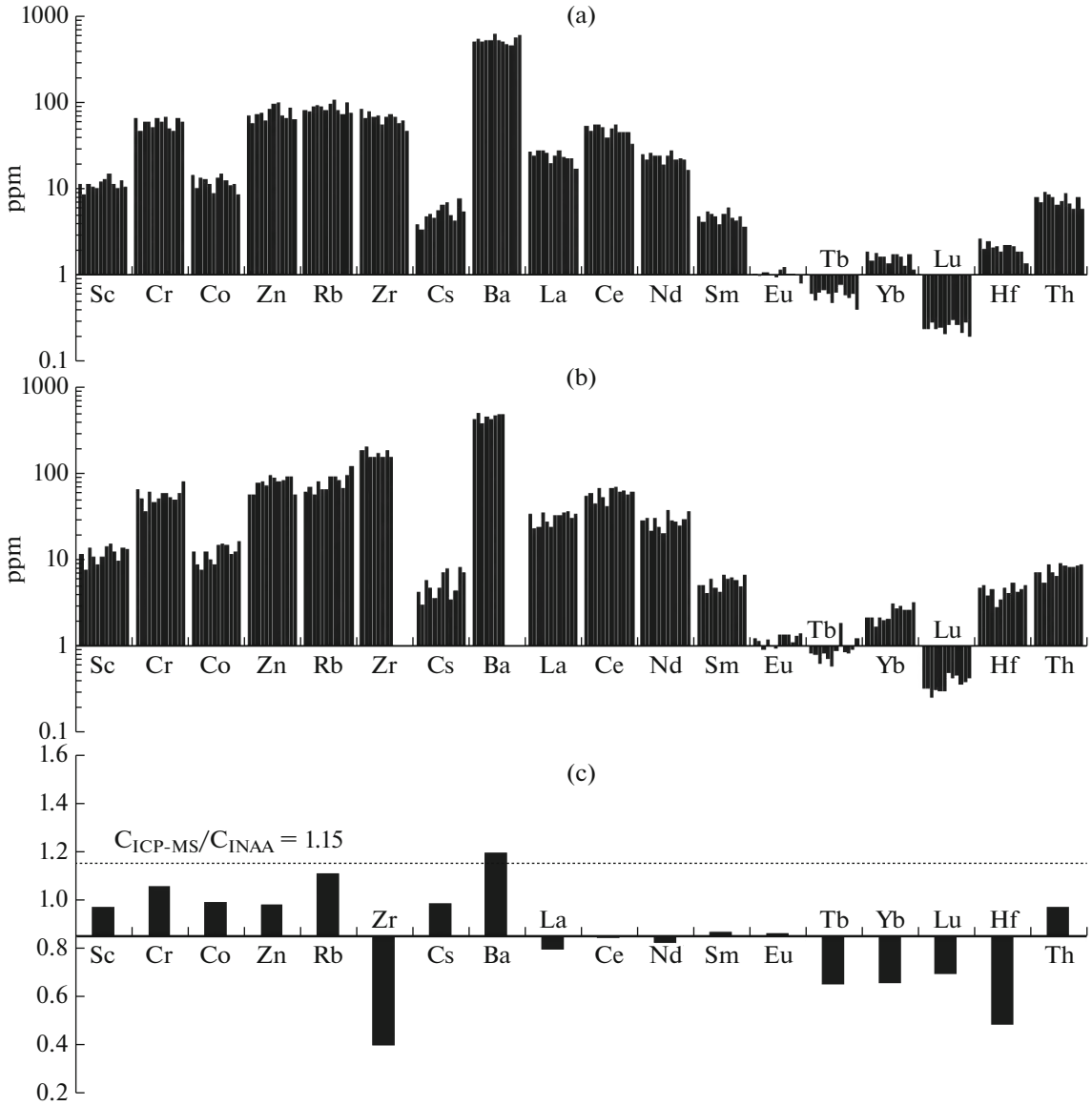

Fig. 5. Contents of rare and trace elements (ppm) in IRS samples determined by ICP-MS (a) and INAA (b) methods, and ratios of average contents of these elements (C_{ICP-MS}/C_{INAA}) (c).

between erosion products of the felsic and mafic magmatic rocks. Diagram $(La/Yb)_N$–$(Eu/Sm)_N$ is the modified version of the $(La/Yb)_N$–Eu/Eu* diagram, where the Eu/Eu* ratio is replaced by the $(Eu/Sm)_N$ ratio (Dubinin, 2006). It is related with the fact that REE data on modern bottom sediments of the Russian Arctic seas reported in the late 1980s–early 1990s are incomplete. The use of Th for plotting the third diagram compensates the presence of only La and Yb contents in the INAA-obtained data. According to (Condie, 1993), average Th contents in the Archean and Proterozoic granites are 15 and 18 ppm, respectively. The Late Proterozoic and Meso-Cenozoic basalts have much lower Th contents: 2.6 and 2.4 ppm, respectively. Hence, the Th content in the suspended particulate matter of rivers and the main parameters of chondrite-normalized REE patterns could be indicators of the composition of rock complexes eroded in the watershed areas.

Analysis of the plots (Fig. 7), firstly, revealed no principle difference in the trace element composition of IRS points from different regions. Secondly, IRS data points in the $(La/Yb)_N$–Eu/Eu* and $(La/Yb)_N$–$(Eu/Sm)_N$ diagrams are mainly restricted to data points of the suspended particulate matter of the Severnaya Dvina, Ob, and Lena, Mackenzie, and Arctic Red rivers. Thirdly, IRS data points in the Th–$(La/Yb)_N$ diagram are confined to the data points of modern bottom deposits of the Omoloi, Yana, Severnaya Dvina, and Ob rivers; i.e., they show slightly dif-

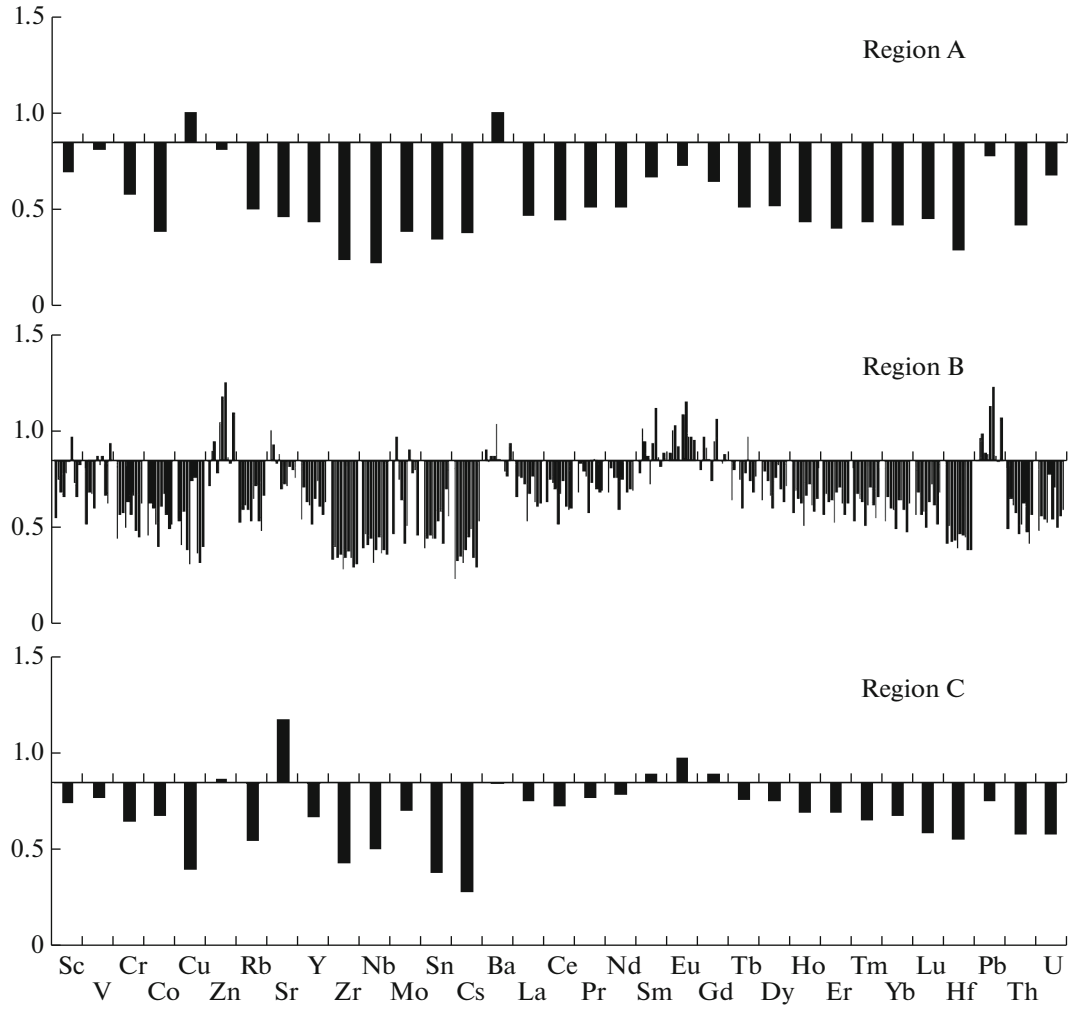

Fig. 6. PAAS-normalized contents of rare and trace elements in IRS samples from regions A, B, and C (Fig. 1). Number of columns in element cells corresponds to the number of analyzed samples.

ferent distribution as compared to those in two other plots. It is also noteworthy that IRS data points from regions A and B in two other diagrams are localized closely to each other. In contrast, IRS data points from region A in the third diagram are confined to the average composition of river fans with definite contribution of mafic volcanic rocks, while IRS data from region B have slightly more mature composition. Hence, the analyzed IRS samples are erosion products of both mafic and felsic magmatic and/or sufficiently mature sedimentary rocks (i.e., samples of all four regions show no predominance of definite rock complex in a provenance).

Figure 8 shows only distribution of IRS data points according to the INAA data and data points of the average composition of the suspended particulate matter of the Russian and Canadian Arctic rivers in the $(La/Yb)_N$–$(Eu/Sm)_N$ and $(La/Yb)_N$–Th diagrams. The IRS data points in the $(La/Yb)_N$–$(Eu/Sm)_N$ diagram show sufficiently compact distribution. Most IRS data points from regions A and B are localized near average compositions of the bottom sediments of the Severnaya Dvina, Ob, Mackenzie, and Arctic Red rivers. The IRS data points from region C are shifted toward higher $(La/Yb)_N$ and $(Eu/Sm)_N$ ratios relative to the main data set, being closer to the ratios in bottom sediments of the Lena River. In the $(La/Yb)_N$–Th diagram, IRS data points are restricted to average compositions of the bottom sediments of the Severnaya Dvina, Ob, Yana, and Omoloi rivers. However some IRS samples from region B presumably have a significant contribution of the geochemically immature material. It is pertinent to once more mention that based on ICP-MS and INAA data, the geochemical characteristics of the ice-rafted IRS collected from four regions (except for those of samples XIV/1a-12 and XIV/1a-17) are inconsistent with their derivation through the erosion of mafic magmatic rocks and incorporation in ice in the central and eastern Kara Sea and in the western Laptev Sea.

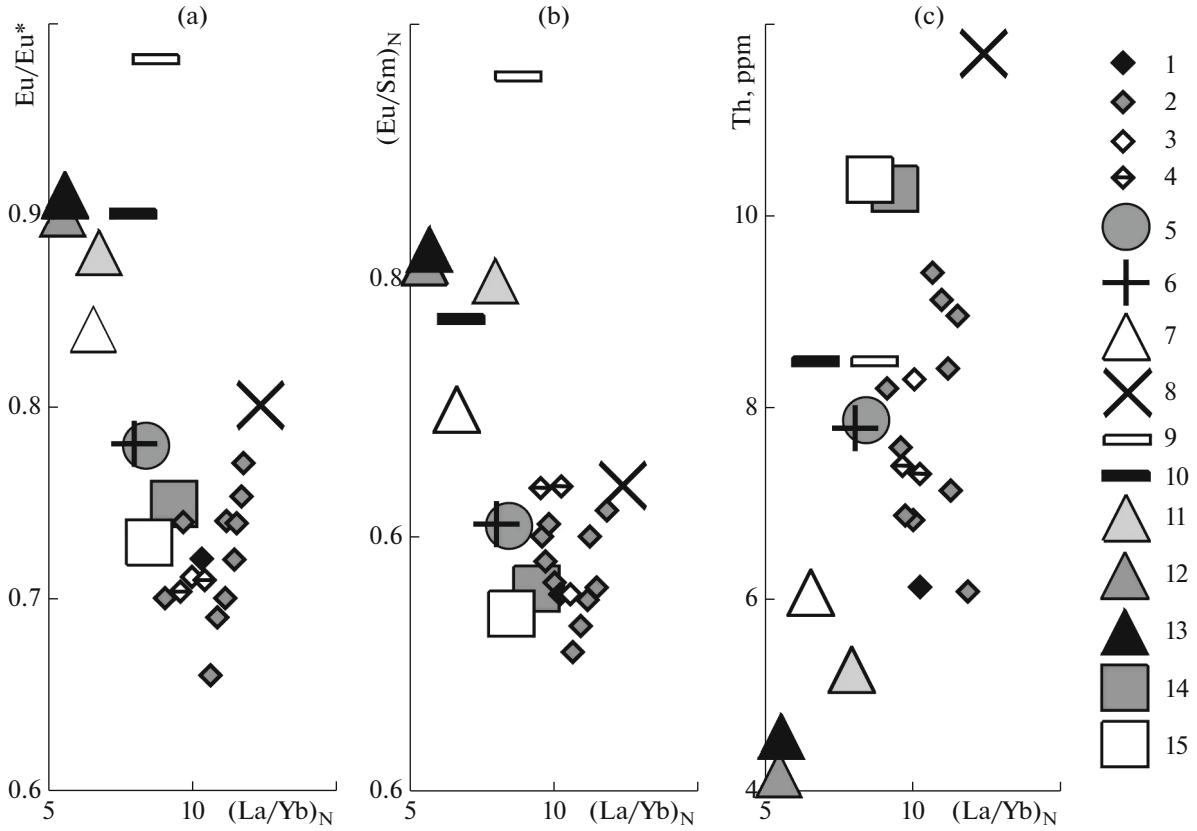

Fig. 7. Distribution of IRS data points from different Arctic regions (trace element contents were determined by ICP-MS) and data points of the average composition of modern bottom sediments of the large Arctic rivers in the $(La/Yb)_N$–Eu/Eu* (a), $(La/Yb)_N$–$(Eu/Sm)_N$ (b), and $(La/Yb)_N$–Th (c) diagrams. (1) IRS from region A; (2) IRS from region B; (3) IRS from region C; (4) IRS from region D (Yermak Plateau); (5) North Dvina River; (6) Ob River; (7) Yenisei River; (8) Lena River; (9) Yana River; (10) Omoloi River; (11) Khatanga River; (12) Kheta River; (13) Kotui River; (14) Mackenzie River; (15) Arctic Red River.

The Th/Co–La diagram plotted for ICP-MS data (Fig. 9) also makes it possible to reconstruct the source rock complexes of the studied IRS samples. It is seen in the diagram that the data points of IRS samples from regions A and C correspond to different La contents, while the data points of samples collected in region B occupy mainly an intermediate position. Most IRS samples are localized in the considered plot near average compositions of modern bottom sediments of the Severnaya Dvina, Omoloi, and Ob rivers. The IRS samples with insignificant La content (samples from region A and sample XIV/1a-17 from region B) are comparable with modern sediments of rivers draining the mafic magmatic rocks. However, the Th/Co ratios in these samples are much higher than those in sediments of the Yenisei and Khatanga rivers, the drainage areas of which are mainly made up of mafic magmatic rocks. Based on the La content and Th/Co ratio, the considered data set can be estimated as formed through the decomposition of both mafic and felsic magmatic and/or sufficiently mature sedimentary rocks, because data points of these samples in the Th/Co–La diagram are plotted approximately in the middle between PAAS and the average composition of Meso-Cenozoic basalts (Condie, 1993). This agrees with conclusions obtained by analyzing $(La/Yb)_N$–Eu/Eu*, $(La/Yb)_N$–$(Eu/Sm)_N$, and $(La/Yb)_N$–Th diagrams.

Data points of IRS samples from regions A, B, and C were plotted in the Si/Al–Ce and Si/Al–Sr diagrams together with the composition fields of surface bottom sediments of the East Siberian, Chukchi, and Laptev seas (Viscosi-Shirley, 2001). Virtually all IRS data points are accumulated in the overlap area of modern sediments of the Laptev and East Siberian seas, being located between data points of the average basalts and shales and frequently confined to the latters (Fig. 10). It is noteworthy that the data points of IRS samples from region A fall relatively close to the average composition of basalts in the first of the plots and shows no confinement to any of average data points in the second plot.

It is seen in the Si/Al–Ce diagram that IRS data points are plotted in the field between average compositions of modern bottom sediments of the Severnaya Dvina, Ob, Yana, Mackenzie, and Arctic Red rivers, on the one hand, and modern bottom sediments of the

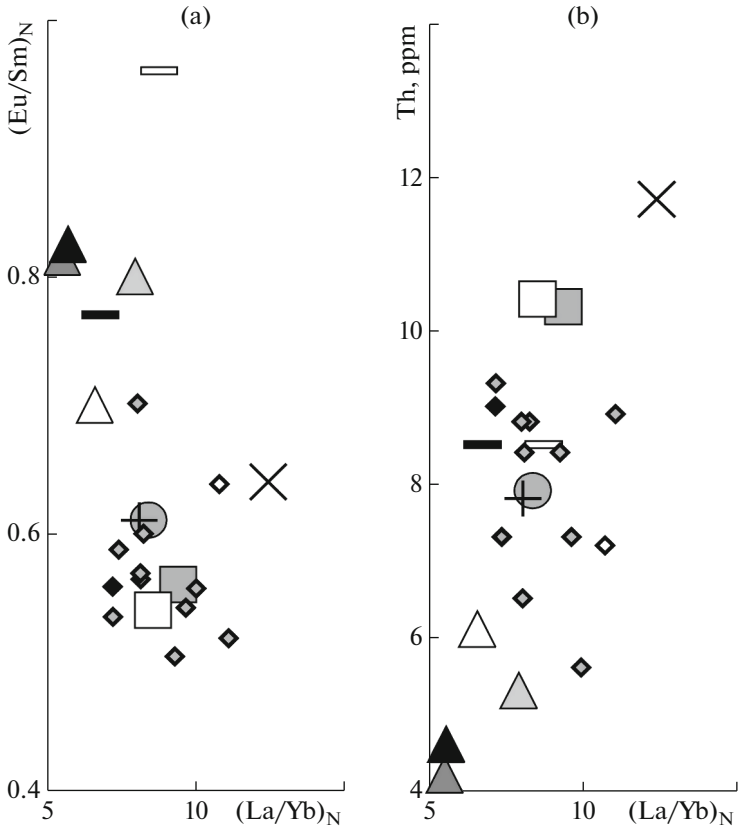

Fig. 8. Distribution of IRS data points from different Arctic regions (trace element contents were determined by the INAA method) and data points of average compositions of modern bottom sediments from the large Arctic rivers in the $(La/Yb)_N$–$(Eu/Sm)_N$ (a) and $(La/Yb)_N$–Th (b) diagrams. Symbols are shown in Fig. 7.

Lena River, on the other, which are characterized by the mature composition of sediments. The same position of IRS data points from regions A, B, and C is observed in the Si/Al–Sr diagram, except for IRS sample from region C, which is located near the average sediment of the Yenisei River (Fig. 11).

DISCUSSION AND CONCLUSIONS

Before examining the obtained results, let us consider briefly the results of previous studies. According to (Wahsner et al., 1999), surface sediments of the Barents Sea are characterized by the illite–chlorite–kaolinite–smectite (in order of decreasing content) assemblage of clay minerals. Modern bottom sediments confined to the Franz Josef Land and Novaya Zemlya archipelagoes are characterized by the sufficiently wide composition of clay rocks, which is caused by the diversity of rocks exposed on the archipelagoes. In the vicinity of the Franz Jozef Land archipelago, clay minerals of modern bottoms sediments are dominated by smectite and kaolinite (Nürnberg et al., 1995; Stein et al., 1994), which is related to the erosion of sedimentary rocks and basalts subjected to chemical weathering in the Mesozoic. Nürnberg et al. (1994) believe that the Franz Jozef Land archipelago is the main kaolinite source in the Eurasian basin, whereas Novay Zemlya is the main illite supplier. The mixing of the Arctic and North Atlantic waters in the eastern Barents Sea leads to the formation of large cyclonic gyre, which affects the distribution of clay mineral assemblages (Nürnberg et al., 1995). Sediments have higher smectite content in areas with the North Atlantic waters emptying into the Barents Sea, whereas sediments precipitated by the Arctic waters have much lower content of this mineral. According to (Wahsner et al., 1999), the smectite content in the region south of Spitsbergen is no more than 10% (hereinafter, of the total clay minerals present in sediment). At the same time, the Barents Sea is characterized by sufficiently deep-water shelf, which, according to (Elverhoi et al., 1989; Nürnberg et al., 1994; Pfirman et al., 1990) could not be the source of significant IRS content. Modern bottom sediments of the western Kara Sea have low contents of chlorite and kaolinite. Sediments from its central and eastern parts show elevated contents of smectite and illite (Dethleff and Kuhlmann, 2010; Gorbunova, 1997; Wahsner et al., 1999;), while all clay minerals are ascribed to the smectite–illite–chlorite–kaolinite assemblage (Wahsner

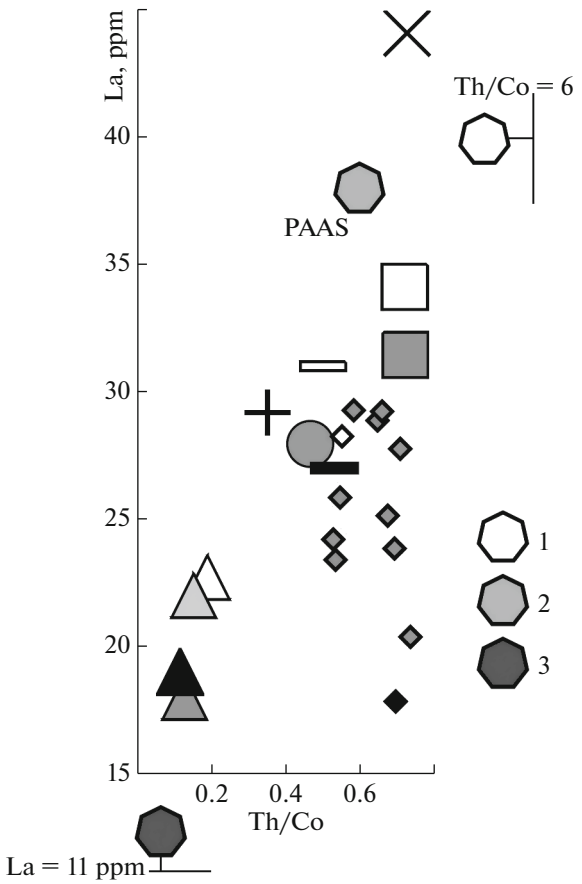

Fig. 9. Distribution of bulk compositions of IRS samples from different Arctic regions (trace element contents were determined by the ICP-MS method), data points of average compositions of modern bottom sediments of the large Arctic rivers, as well as the Meso-Cenozoic average basalts, average Phanerozoic granites, and PAAS in the Th/Co–La diagram. (1) Average Phanerozoic granites; (2) PAAS; (3) average Meso-Cenozoic basalts (Condie, 1993). Other symbols are shown in Fig. 7.

et al., 1999). The highest smectite contents (from 40 to 70%) were found in the Yenisei River estuary (Gorbunova, 1997; Lein et al., 2013; Nürnberg et al., 1995; Wahsner et al., 1999). According to (Asadulin et al., 2015), the eastern Kara Sea is dominated by the terrigenous material transported by the Ob river waters.

Serova and Gorbunova (1997) indicate that the clay fraction in the surface bottom sediments of the Laptev Sea consists mainly of illite (60–70%) and chlorite (20–30%). According to (Dethleff and Kuhlmann, 2010; Nürnberg et al., 1994; Silverberg, 1972; Stein et al., 1994; and others), the clay fraction of sediments in the western Laptev Sea contains significant amount of smectite (~26%), and slightly lowered illite content as compared to most of other Arctic Seas. The kaolinite and chlorite contents in these sediments are comparable with those in sediments of the eastern Laptev Sea. Most authors believe that precisely ice from the western Laptev Sea served as source of the elevated smectite contents in the region north of Spitsbergen (Nürnberg et al., 1994; Stein et al., 1994). Modern bottom sediments of the eastern Laptev Sea, in contrast, have high illite fraction (Dethleff and Kuhlmann, 2010; Wahsner et al., 1999).

The studies by Kalinenko et al. (1996) showed that shelf sediments of the East Siberian Sea are characterized by the illite–smectite–chlorite–kaolinite assemblage of clay minerals. Sediments of the East Siberian Sea, as those of Beaufort Sea, have sufficiently low smectite contents (Naugler, 1967; Silverberg, 1972). According to (Khim, 2003; Logvinenko and Ogorodnikov, 1980; Stein et al., 1994), modern sediments of the East Siberian and Chukchi seas contain significant fraction of illite of the illite–chlorite–kaolinite–smectite assemblage (Wahsner et al., 1999). Its main source is the Kolyma River (Khim, 2003). Significant amount of smectite and kaolinite is supplied together with the Bering Sea waters to the Chukchi Sea, especially, its western part (Khim, 2003). The main source of smectite is the Yukon River (McManus et al., 1974; Naidu and Mowatt, 1983; and others). An increase of chlorite content, in some cases, up to 40% is observed in the coastal part of the Chukchi Sea, including areas in front of the mouths of some rivers (Wahsner et al., 1999).

Modern bottom sediments of the Beaufort Sea have elevated contents of kaolinite, whose sources are Meso-Cenozoic rocks of northern Alaska and islands of the Canadian Archipelago (Dalrymple and Maass, 1987; Darby, 1975; Stein et al., 1994).

Average contents of clay minerals in the surface sediments of the Russian Arctic seas are summarized in (Wahsner et al., 1999) (Table 4). It is considered that the composition of clay mineral assemblage under conditions of suppressed chemical weathering and weakly expressed diagenetic processes reflects mainly the composition of drainage areas of the large Russian and Canadian Arctic rivers (Darby et al., 1989; Lisitzin, 1994, 2010; Stein et al., 1994; Wahsner et al., 1999; and others).

The differences in clay mineral assemblages, which were revealed in geographically close areas, are likely caused by several reasons: (1) different representativeness of sampling; (2) application of different methods of analysis and interpretation (in particular, the nature of X-ray amorphous matter is difficult to determine and it is frequently accepted as smectite); (3) hydration of micas and chlorite (or chloritized basalts) is accompanied by the subsequent increase of smectite component in the mixed-layer phases (however, this fact is frequently not taken into account). It should also be taken into account that the quantitative estimate of the mineral composition of clays by the complete profile analysis encounters difficulties with a choice of standards.

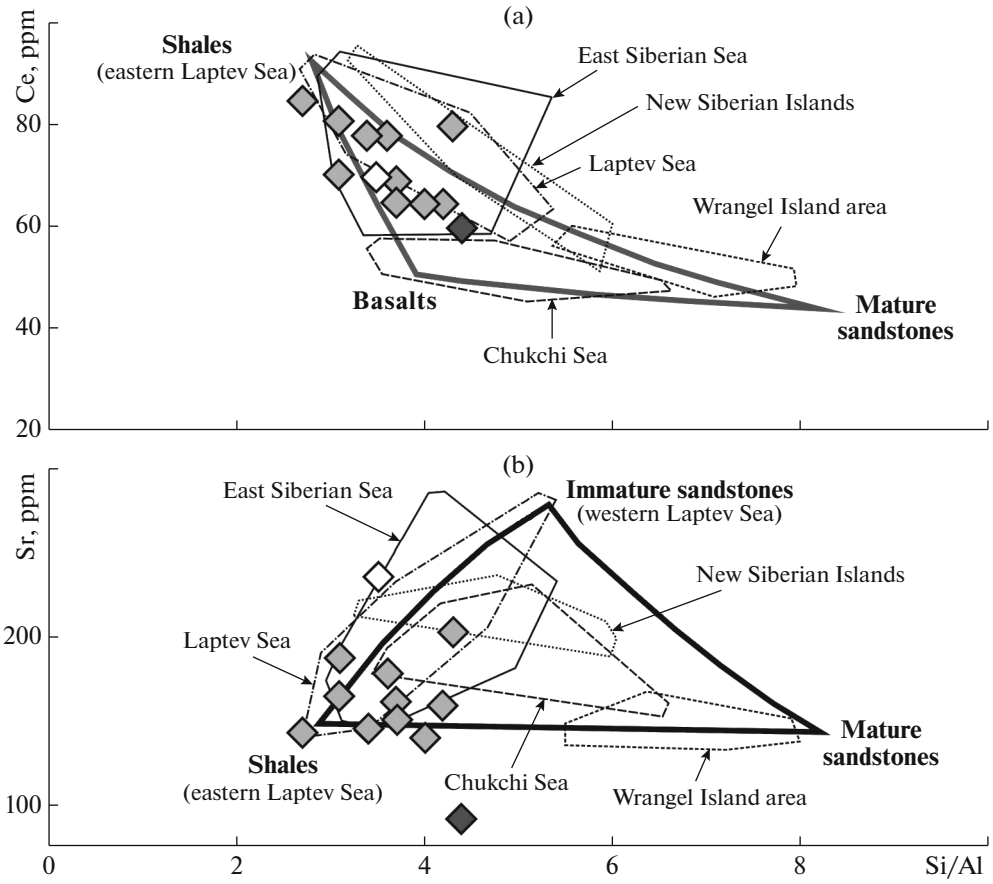

Fig. 10. Distribution of data points of IRS samples from regions A, B, and C in the Si/Al–Ce (a) and Si/Al–Sr (b) diagrams proposed in (Viscosi-Shirley, 2001). Symbols are shown in Fig. 7.

As shown in (Nürnberg et al., 1994), IRS samples collected in the southern/Siberian branch of the Transpolar Drift have high contents of smectite (15–60%), which make them similar with surface bottom sediments on shelves of the Laptev Sea (up to 45% smectite) and Kara Sea (up to 70% smectite). In the author's opinion, precisely Kara and Laptev seas are the potential IRS sources in ices of the southern branch of the Transpolar Drift. This is also confirmed by reconstructions of the ice transport pathways (Pfirman et al., 1997; Wahsner et al., 1999). According to (Dethleff and Kuhlmann, 2010), IRS in ice from the western Fram Strait are depleted in smectite and enriched in illite, which is correlated with the compo-

Table 4. Average contents of different clay minerals in the clay fraction of surface sediments of the Russian Arctic region, after (Wahsner et al., 1999)

Russain Arctic seas	Clay minerals, %			
	Smectite	Illite	Chlorite	Kaolinite
Eastern Barents Sea	15	55	20	10
Western Barents Sea	6	57	20	17
Western Kara Sea	38	38	15	10
Eastern Kara Sea	60	19	12	9
Western Laptev Sea	26	40	22	14
Eastern Laptev Sea	19	49	21	11
East Siberian Sea	4	69	20	8
Chukchi Sea	9	57	25	9

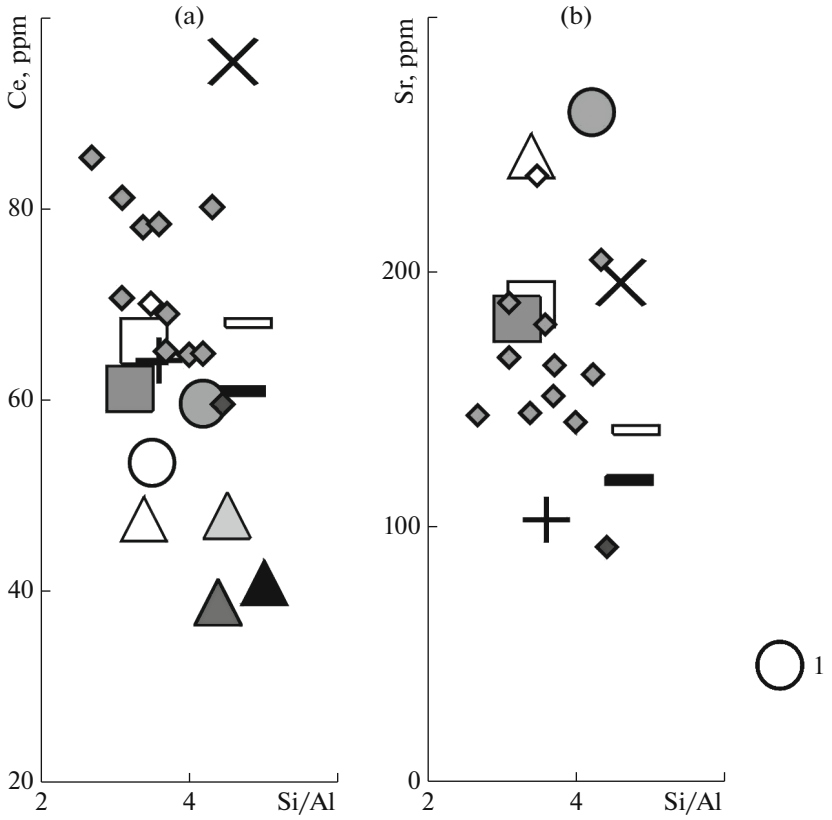

Fig. 11. Distribution of data points of IRS samples from regions A, B, and C and data points of the average composition of modern bottom sediments of some large Arctic rivers in the Si/Al–Ce (a) and Si/Al–Sr (b) diagrams. (1) Average composition of bottom sediments of the Pechora River. Other symbols are shown in Fig. 7.

sition of clay fraction in modern bottom sediments of the eastern Laptev Sea and the Arctic sector of North America. In the eastern Fram Strait, IRS is enriched in smectite and depleted in illite, which is typical of bottom sediments of the western Laptev and Kara seas.

The described differences in clay mineral assemblages between surface sediments in different seas of the Arctic shelf also affect their geochemical characteristics. In particular, according to (Viscosi-Shirley, 2001; Viscosi-Shirley et al., 2003), the Ce content and Si/Al ratios in bottom sediments of the Chukchi Sea make it possible to separate such sources as the "East Laptev clay shales", "basalts of the Chukchi Sea", and "mature sandstones" of Wrangel Island. The Sr distribution indicates the influx of erosion products of the fine-grained clastic material (immature sandstones) to the eastern part of the Laptev Sea and points to the absence of basalts on the watersheds.

Examination of element distribution in sediments of the Ob and Yenisei estuaries allowed Asadulin et al. (2013) to establish that bottom sediments of the Ob and Yenisei rivers are characterized by contrasting geochemical features. These authors believe that this fact can be used to discriminate between the Ob and Yenisei sediments on the Kara Sea shelf. It was emphasized in (Asadulin et al., 2015, p. 209) that "...the floor of the eastern Kara Sea is mainly covered by sediments identified as the Ob sediments. This ... corresponds to the predominant role of the Ob River in the transportation of terrigenous material to the sea ... Samples determined using the geochemical criterion as Yenisei sediments are almost completely localized in the estuary zone, with numerous composition points of unclear affiliation restricted to its distal part."

In recent years, we also attempted to analyze the trace and rare element distribution in ice-rafted sedimentary material. In particular, Shevchenko et al. (2017b) analyzed the distribution of V, Co, Ni, Sr, Nb, and REE in IRS samples collected in the western Arctic region in the Yermak Plateau area (Cruise ARK-XX/3 of R/V *Polarstern*, 2004). It was established that in terms of the Nb and V relationship, they are intermediate between average compositions of the suspended particulate matter of the Yenisei and Khatanga rivers, as well as Meso-Cenozoic basalts, on the one hand, and suspended particulate matter of the Ob, Lena, and PAAS, on the other. This also follows from the REE distribution. It is shown that IRS data points in the Nb–Sr, Ni–Co, and Co–Sr diagrams are mainly confined to average compositions of the suspended partic-

ulate matter of the Ob and Lena rivers, i.e., water arteries draining areas made up mainly of sedimentary rocks. The Nb, Sr, Ni, and Co contents in the IRS are close to PAAS. All these facts suggest that sources of the studied samples were the bottom sediments from the eastern Laptev and East Siberian seas.

Results of the quantitative assessment of mineral compositions of IRS samples from regions A, B, C, and D using the Rietveld method show that the studied samples contain from ~50 to ~80 wt % quartz and feldspars. Correspondingly, the fraction of layer silicates varies from ~20% (sample XIV/1a-15, region B) to approximately 50% (samples XIV/1a-28, region A; XIV/1a-20, region B (Table 1)).

Layer silicates in the studied IRS samples are dominated by micas and their decomposition products (illite and, presumably, some smectites) with significant content of kaolinite, chlorite, and transformation/disintegration products of the latter. According to (Wahsner et al., 1999), the significant (>60%) content of illite and muscovite among layer silicates in most IRS samples suggests that the possible sources of sedimentary material for them were mineralogically similar bottom sediments from the East Siberian and Chukchi seas, as well as likely the eastern Laptev Sea.

The lower illite and muscovite content (~45%) in sediment of sample XIV/1a-17 (region B) as compared to those of other IRS samples likely indicates that its source were sediments from the western Kara Sea or the western Laptev Sea.

Significant fraction of kaolinite in some IRS samples from region B can be related to the sedimentary material from the Beaufort or Chukchi seas, where kaolinite is delivered from the Bering Sea. In our opinion, this fact indirectly indicates that IRS samples from the North Pole area contain heterogeneous material, which could be derived from different and sufficiently far spaced regions of the Russian and Canadian Arctic region. The presence of samples of several groups (see above) among the material collected in region B also supports the above mentioned opinion.

The comparison of average Cr and Co contents in the suspended particulate matter of the Pechora, Ob, Yenisei, Lena, and Mackenzie rivers with concentrations of these elements in bottom sediments of the Barents, East Siberian, Chukchi, Laptev, and Beaufort seas (Shevchenko et al., 2017a) allowed us to draw conclusion that IRS sources in rafted ice of the North Pole area (region B) likely could be eastern areas of the Laptev Sea, shelves of the East Siberian (mainly its eastern part) and Chukchi seas, as well as of the Beaufort Sea. The $(La/Yb)_N$ ratio in IRS from region B corresponds both to the average value of this parameter in the suspended particulate matter of the Mackenzie and Arctic Red rivers and to $(La/Yb)_{N\ average}$ for crystalline rocks of the Canadian Shield. The $(La/Yb)_N$ ratio in IRS from region B is close to that in the particulate matter of the Yana and Lena rivers. According to (Darby, 2003), this fact can indicate that the IRS from the North Pole area contains material borrowed from the shelf of the eastern Laptev Sea.

At the same time, conclusions made from the bulk X-ray diffraction patterns can be considered as approximate. More reliable results would be obtained by the classical study of <1 μm fraction extracted from all samples, but this is impossible due to the low amount of material.

Positions of IRS data points in the diagrams $(La/Yb)_N$–Eu/Eu*, $(La/Yb)_N$–$(Eu/Sm)_N$, and $(La/Yb)_N$–Th show that the studied samples contain the erosion products of both mafic and felsic magmatic and/or sufficiently mature sedimentary rocks. Examination of geochemical features of most IRS samples from all studied regions suggests that they contain no significant fraction of particulate matter extracted by ice in the eastern Kara Sea or western Laptev Sea, i.e., in the regions where modern bottom sediments are enriched in the erosion products of mafic magmatic rocks. This conclusion is also confirmed by the localization of IRS points in the Th/Co–La, Si/Al–Ce, and Si/Al–Sr diagrams.

Thus, the carried out studies did not provide unambiguous answer to the question concerning the sources of IRS, samples of which were collected from drifting ice in four regions of the Arctic Ocean, but they highlighted some constraints to solve this problem.

ACKNOWLEDGMENTS

We are grateful to the crew of the R/V *Polarstern* and participants of expeditions ARK-XIV/1a and ARK-XX/3 for their help in sampling. A.N. Novigatskii and N.A. Kukina are thanked for help in the preliminary treatment of data, while Academician A.P. Lisitzin and Professor R. Stein are thanked for supporting this work. Figures were drawn by N.S. Glushakova.

This work was financially supported by the RSF grant 14-50-00095 and project UrO RAN 15-15-5-4.

REFERENCES

Andrews, J.T. and Eberl, D.D., Quantitative mineralogy of surface sediments on the Iceland shelf, and application to down-core studies of Holocene ice-rafted sediments, *J. Sediment. Res.*, 2007, vol. 77, pp. 469–479.

Andrews, J.T. and Eberl, D.D., Determination of sediment provenance by unmixing the mineralogy of source-area sediments: the "SedUnMix" program, *Mar. Geol.*, 2012, vol. 291, pp. 24–33.

Andrews, J.T. and Hardardottir, J., A comparison of Holocene sediment- and paleomagnetic characteristics from the margins of Iceland and East Greenland, *Jokull*, 2009, vol. 59, pp. 51–66.

Arctic '98: The Expedition ARK-XIV/1a of RV "Polarstern" in 1998, Jokat, W., Ed., in *Berichte Polarforsch.*, 1999, vol. 308.

Asadulin, En.E., Miroshnikov, A.Yu., and Velichkin, V.I., Geochemical Signature of Bottom Sediments in the Mixing Zones of Ob and Yenisei Waters with Kara Sea Water, *Geochem. Int.* 2013, no. 12, pp. 1005–1018.

Asadulin, En.E., Miroshnikov, A.Yu., Usacheva, A.A., and Velichkin, V.I., Geochemical recognition of terrigenous material from the Ob and Yenisei rivers in bottom sediments of the eastern part of the Kara Sea, *Dokl. Earth. Sci.*, 2015, vol. 461, no. 2, pp. 270–272.

Bayon, G., Toucanne, S., Skonieczny, C., et al., Rare earth elements and neodymium isotopes in world river sediments revisited, *Geochim. Cosmochim. Acta*, 2015, vol. 170, pp. 17–38.

Bobrov, V.A., Granina, L.Z., Kolmogorov, Yu.P., and Melgunov, M.S., Minor elements in aeolian and riverine suspended particles in Baikal region, *Nucl. Instr. Methods Phys. Res.*, 2001, vol. 470, pp. 431–436.

Bobrov, V.A., Khodzher, T.V., Granina, L.Z., et al., Rare earth elements in the eolian and riverine suspended material in the Lake Baikal region, *Geol. Geofiz.*, 2001, vol. 42, pp. 267–277.

Colony, R.L., Rigor, I., and Runciman-Moore, K., A summary of observed ice motion and analyzed atmospheric pressure in the Arctic basin, 1979–1990, in *Appl. Physics Lab.*, Seattle: Univ. Wash., 1991, pp. 13–91.

Condie, K.C., Chemical composition and evolution of the upper continental crust: contrasting results from surface samples and shales, *Chem. Geol.*, 1993, vol. 104, pp. 1–37.

Dalrymple, R.W. and Maass, O.C., Clay mineralogy of Late Cenozoic sediments in the CESAR cores, Alpha Ridge, central Arctic Ocean, *Can. J. Earth Sci.*, 1987, vol. 24, pp. 1562–1569.

Darby, D.A., Kaolinite and other clay minerals in Arctic Ocean sediments, *J. Sediment. Petrol.*, 1975, vol. 45, pp. 272–279.

Darby, D.A., Sources of sediment found in sea ice from the western Arctic Ocean, new insights into processes of entrainment and drift patterns, *J. Geophys. Res.: Oceans*, 2003, vol. 108, no. C8.

Darby, D.A., Naidu, A.S., Mowatt, T.C., and Jones, G., Sediment composition and sedimentary processes in the Arctic Ocean, in *The Arctic Seas—Climatology, Oceanography, Geology and Biology*, Herman, Y., Ed., New York: Van Nostrand Reinhold Co., 1989, pp. 657–720.

Darby, D.A., Myers, W.B., Jakobsson, M., and Rigor, I., Modern dirty sea ice characteristics and sources: the role of anchor ice, *J. Geophys. Res.*, 2011, vol. 116. C09008. https://doi 10.1029/2010JC006675

Dethleff, D. and Kuhlmann, G., Fram Strait sea-ice sediment provinces based on silt and clay compositions identify Siberian Kara and Laptev seas as main source areas, *Polar Res.*, 2010, vol. 29, pp. 265–282.

Dethleff, D., Nurnberg, D., Reimnitz, E., et al., East Siberian Arctic Region Expedition'92: the Laptev Sea—its significance for Arctic Sea-ice formation and transpolar sediment flux, *Ber. Polarforsch.*, 1993, vol. 120, pp. 3–44.

Dubinin, A.V., *Geokhimiya redkozemel'nykh elementov v okeane* (Geochemistry of Rare Earth Elements in the Ocean), Moscow: Nauka, 2006.

Eicken, H., Reimnitz, E., Alexandrov, V., et al., Sea-ice processes in the Laptev Sea and their importance for sediment export, *Contin. Shelf Res.*, 1997, vol. 17, pp. 205–233.

Elverhoi, A., Pfirman, S., Solheim, A., and Larssen, B.B., Glaciomarine sedimentation in epicontinental seas exemplified by the northern Barents Sea, *Mar. Geol.*, 1989, vol. 85, pp. 225–250.

Emeis, K., Particulate suspended matter in major world rivers-II: results on the rivers Indus, Waikato, Nile, St. Lawrence, Yangtze, Parana, Orinoco, Caroni and Mackenzie, *Mitt. Geol.-Palaont. Inst.*, Univ. Hamburg, 1985, no. 58, pp. 593–617.

Farmer, G.L., Licht, K., Swope, R.J., and Andrews, J.T., Isotopic constraints on the provenance of fine-grained sediment in LGM tills from the Ross Embayment, Antarctica, *Earth Planet. Sci. Lett.*, 2006, vol. 249, pp. 90–107.

Gaillardet, J., Dupre, B., and Allegre, C.J., Geochemistry of large river suspended sediments: silicate weathering or recycling tracer?, *Geochim. Cosmochim. Acta*, 1999, vol. 63, nos. 23/24, pp. 4037–4052.

Gel'man, E.M. and Starobina, I.Z., *Fotometricheskie metody opredeleniya porodoobrazuyushchikh elementov v rudakh, gornykh porodakh i mineralakh* (Photometric Methods for the Determination of Major Elements in Ores, Rocks, and Minerals), Moscow: GEOKhI AN SSSR, 1976.

Gorbunova, Z.N., Clay-size minerals in the Kara Sea sediments, *Oceanology*, 1997, vol. 37, no. 5, pp. 709–712.

Gordeev, V.V., Rachold, V., and Vlasova, I.E., Geochemical behaviour of major and trace elements in suspended particulate material of the Irtysh River, the main tributary of the Ob River, Siberia, *Appl. Geochem.*, 2004, vol. 19, pp. 593–610.

Grousset, F.E., Cortijo, E., Huon, S., et al., Zooming in on Heinrich layers, *Paleoceanography*, 2001, vol. 16, pp. 240–259.

Hemming, S.R., Vorren, T.O., and Kleman, J., Provinciality of ice rafting in the North Atlantic: Application of $^{40}Ar/^{39}Ar$ dating of individual ice rafted hornblende grains, *Quat. Int.*, 2002, vol. 95–96, pp. 75–85.

Herman, Y., *The Arctic Seas – Climatology, Oceanography, Geology, and Biology*, New York: Van Nostrand Reinhold, 1989.

Kalinenko, V.V., Shelekhova, E.S., and Wahsner, M., Clay minerals in the surface sediments of the East Siberian and Laptev Sea, in *Surface-Sediment Composition and Sedimentary Processes in the Central Arctic Ocean and along the Eurasian Continental Margin*, Stein, R., Ivanov, G., Levitan, M., and Fahl, K., Eds., *Rep. Polar Res.* 1996, vol. 212, pp. 43–50.

Kassens, H. and Thiede, J., Climatological significance of Arctic Sea ice at present and in the past, in *Russian-German Cooperation in the Siberian shelf seas: geo-system Laptev-Sea*, Kassens, H., Eds., *Ber. Polarforsch*, 1994, vol. 144, pp. 81–85.

Khim, B.K., Two modes of clay-mineral dispersal pathways on the continental shelves of the East Siberian Sea and western Chukchi Sea, *Geosci. J.*, 2003, vol. 7, pp. 253–262.

Kolatschek, J., Eicken, H., Alexandrov, V.Yu., and Kreyscher, M., The sea ice cover of the Arctic Ocean and the Eurasian marginal seas: a brief overview of present day patterns and variability, in *Surface-Sediment Composition and Sedimentary Processes in the Central Arctic Ocean and along the Eurasian Continental Margin*, Stein, R., Ivanov, G.I., Levitan, M.A., and Fahl, K., Eds., *Ber. Polarforsch*, 1996, vol. 212, pp. 2–19.

Konta, J., Mineralogy and chemical maturity of suspended matter in major rivers sampled under the SCOPE/UNEP project, *Mitt. Geol.-Palaont. Inst.*, Univ. Hamburg, 1985, no. 58, pp. 569–592.

Kontorovich, A.E., Forms of the migration of elements in rivers of the humid zone (based on materials from West Siberia and other regions), in *Geokhimiya osadochnykh porod i rud* (Geochemistry of Sedimentary Rocks and Ores), Moscow: Nauka, 1968, pp. 88–101.

Lein, A.Yu., Makkaveev, P.N., Savvichev, A.S., et al., Transformation of suspended particulate matter into sediment in the Kara Sea in September of 2011, *Oceanology*, 2013, vol. 53, no. 5, pp. 570–606.

Levitan, M.A., Lavrushin, Yu.A., and Stain, R., *Ocherki istorii sedimentatsii v Severnom Ledovitom okeane i moryakh Subarktiki v techenie poslednikh 130 tys. let* (History of Sedimentation in the Arctic Ocean and Subarctic Seas in the Last 130 ka), Moscow: GEOS, 2007.

Lisitzin, A.P., *Ledovaya sedimentatsiya v Mirovom okeane* (Ice Sedimentation in the World Ocean), Moscow: Nauka, 1994.

Lisitzin, A.P., *Sea-Ice and Iceberg Sedimentation in the Ocean: Recent and Past,* Berlin: Springer, 2002.

Lisitzin, A.P., A new type of sedimentogenesis in the Arctic (marine ice): New approaches to the study of processes, *Geol. Geofiz.*, 2010, vol. 51, no. 1, pp. 18–60.

Lisitzin, A.P. and Shevchenko, V.P., Glaciomarine sedimentation, in *Encyclopedia of Marine Geosciences*, Harff, J., Meschede, M., Petersen, S., and Thiede, J., Eds., Dordrecht: Springer, 2016, pp. 288–294.

Lisitzin, A.P., Gurvich, E.G., Lukashin, V.N., et al., *Geokhimiya elementov-gidrolizatov* (Geochemistry of Hydrolyzate Elements), Moscow: Nauka, 1980.

Logvinenko, N.V. and Ogorodnikov, V.I., Recent bottom sediments on the Chukchi Sea shelf, *Okeanologiya*, 1980, vol. 20, no. 4, pp. 681–687.

Martin, J.M. and Meybeck, M., Chemical composition of river-borne particulates, *Mar. Chem.*, 1979, vol. 7, no. 2, pp. 193–206.

McManus, D.A., Venkatarathnam, K., Hopkins, D.M., and Nelson, H.C., Yukon River sediment on the northernmost Bering Sea shelf, *J. Sediment. Petrol.*, 1974, vol. 44, pp. 1052–1060.

Moros, M., McManus, J., Rasmussen, T., et al., Quartz content and the quartz-to-plagioclase ratio determined by X-ray diffraction: proxies for ice rafting in the northern North Atlantic?, *Earth Planet. Sci. Lett.*, 2004, vol. 218, pp. 389–401.

Morozov, N.P., Baturin, G.N., Gordeev, V.V., and Gurvich, E.G., The composition of suspended material and sediments at estuaries of the northern Dvina, Mezen, Pechora, and Ob rivers, *Gidrokhim. Mater.*, 1974, vol. 60, pp. 60–73.

Naidu, A.S. and Mowatt, T.C., Sources and dispersal patterns of clay minerals in surface sediments from the continental shelf areas off Alaska, *GSA Bull.*, 1983, vol. 94, pp. 841–854.

Naugler, F.P., Recent sediments of the East Siberian Sea, *M.S. Thesis*, Univ. Wash. DC, 1967.

Nürnberg, D., Wollenburg, I., Dethleff, D., et al., Sediments in Arctic Sea ice: Implications for entrainment, transport and release, *Mar. Geol.*, 1994, vol. 119, pp. 185–214.

Nürnberg, D., Levitan, M.A., Pavlidis, J.A., and Shelekhova, E.S., Distribution of clay minerals in surface sediments from the eastern Barents and south-western Kara seas, *Geol. Rundsch*, 1995, vol. 84, pp. 665–682.

Pfirman, S., Lange, M.A., Wollenburg, I., and Schlosser, P., Sea ice characteristics and the role of sediment inclusions in deep-sea deposition: Arctic-Antarctic comparisons, in *Geological History of the Polar Oceans: Arctic versus Antarctic*, Bleil, U. and Thiede, J., Eds., Dordrecht: Kluwer Acad. Publ., 1990, pp. 187–211.

Pfirman, S.L., Eicken, H., Bauch, D., and Weeks, W.F., The potential transport of pollutants by Arctic Sea ice, *Sci. Tot. Envir.*, 1995, vol. 159, pp. 129–146.

Pfirman, S.L., Colony, R., Nürnberg, D., et al., Reconstructing the origin and trajectory of drifting Arctic Sea ice, *J. Geophys. Res.*, 1997, vol. 102, pp. 12575–12586.

Pirrung, M., Fütterer, D., Grobe, H., et al., Magnetic susceptibility and ice-rafted debris in surface sediments of the Nordic Seas: Implications for Isotope Stage 3 oscillations, *Geo-Mar. Lett.*, 2002, vol. 22, pp. 1–11.

Rachold, V., Major, trace and rare earth element geochemistry of suspended particulate material of East Siberian rivers draining to the Arctic Ocean, in *Land-Ocean Systems in the Siberian Arctic: Dynamics and History*, Berlin: Springer, 1999, pp. 1999–222.

Rachold, V., Alabyan, A., Hubberten, H.-W., et al., Sediment transport to the Laptev Sea - hydrology and geochemistry of the Lena River, *Polar Res.*, 1996, vol. 15, no. 2, pp. 183–196.

Reimnitz, E., Dethleff, D., and Nurnberg, D., Contrasts in Arctic shelf sea-ice regimes and some implications: Beaufort Sea versus Laptev Sea, *Mar. Geol.*, 1994, vol. 119, pp. 215–225.

Rentgenografiya osnovnykh tipov porodoobrazuyushchikh mineralov (X-ray Diffraction Analysis of the Major Types of Rock-Forming Minerals), Leningrad: Nedra, 1983, p. 360.

Savenko, V.S., *Khimicheskii sostav vzveshennykh nanosov rek Mira* (The Chemical Composition of Suspended Material in Rivers of the World), Moscow: GEOS, 2006.

Savenko, V.S., Pokrovskii, O.S., Dyupre, B., and Baturin, G.N., Chemical composition of suspended material in large rivers of Russia and adjacent countries, *Dokl. Earth Sci.*, 2004, vol. 398, no. 1, pp. 938–942.

Scientific Cruise Report of the Arctic Expedition ARK-XX/3 of RV "Polarstern" in 2004: Fram Strait, Yermak Plateau and East Greenland Continental Margin, Stein, R., Ed., *Berichte Polar Meeresforsch.*, 2005, vol. 517.

Serova, V.V. and Gorbunova, Z.N., Mineral composition of soils, aerosols, suspended matter, and bottom sediments of the Lena River estuary and the Laptev Sea, *Oceanology*, 1997, vol. 37, no. 1, pp. 121–125.

Shevchenko, V.P., Lisitsyn, A.P., Polyakova, E.I., et al., Distribution and composition of sedimentary material in the snow cover of the Arctic drift ice (Fram Strait), *Dokl. Earth Sci.*, 2002, vol. 383, no. 3, pp. 278–281.

Shevchenko, V.P., Maslov, A.V., Lisitzin, A.P., et al., Elemental composition of the sedimentary material in drifting ice of the Arctic, in *Geografiya polyarnykh regionov. Ser, voprosy geografii* (Geography of Polar Regions: Ser. Issues

of Geography), Kotlyakov, V.M., Ed., Moscow: Dom Kodeks, 2016, pp. 390–413.

Shevchenko, V.P., Maslov, A.V., Lisitzin, A.P., et al., Systematics of Cr, Co, and REE in the sedimentary material of drifting ices in the northern Beaufort Gyre, *Litosfera*, 2017a, no. 3, pp. 59–70.

Shevchenko, V.P., Maslov, A.V., and Stein, R., Distribution of some rare and trace elements in ice-rafted sediments in the Yermak Plateau area, Arctic Ocean, *Oceanology*, 2017b, vol. 57, no. 6, pp. 855–863.

Silverberg, N., Sedimentology of the surface sediments of the East Siberian and Laptev seas, *Ph.D. Thesis*, Univ. Wash., DC, 1972.

Stein, R., Grobe, H., and Wahsner, M., Organic carbon, carbonate, and clay mineral distributions in eastern central Arctic Ocean surface sediments, *Mar. Geol.*, 1994, vol. 119, pp. 269–285.

Taylor, S.R. and McLennan, S.M., *The Continental Crust: Its Composition and Evolution*, Oxford: Blackwell 1985. Translated under the title *Kontinental'naya kora, ee sostav i evolyutsiya*, Moscow: Mir, 1988.

Verplanck, E.P., Farmer, G.L., Andrews, J., et al., Provenance of Quaternary glacial and glaciomarine sediments along the southeast Greenland margin, *Earth Planet. Sci. Lett.*, 2009, vol. 286, pp. 52–62.

Viscosi-Shirley, C., Siberian-Arctic shelf surface-sediments: Sources, transport pathways and processes, and diagenetic alteration, *PhD Thesis*, Oregon State Univ., 2001.

Viscosi-Shirley, C., Pisias, N., and Mammone, K., Sediment source strength, transport pathways and accumulation patterns on the Siberian-Arctic's Chukchi and Laptev shelves, *Cont. Shelf Res.*, 2003, vol. 23, pp. 1201–1225.

Votyakov, S.L., Kiseleva, D.V., Shagalov, E.S., et al., Multielement analysis of geological samples by the ICP-MS method using ELAN 9000, in *Ezhegodnik-2005* (Yearbook-2005), Yekaterinburg: IGG UrO RAN, 2006, pp. 425–430.

Wahsner, M., Muller, C., Stein, R., et al., Clay-mineral distribution in surface sediments of the Eurasian Arctic Ocean and continental margin as indicator for source areas and transport pathways – a synthesis, *Boreas*, 1999, vol. 28, pp. 215–233.

Wollenburg, I., Sediment transport by Arctic Sea ice: the recent load of lithogenic and biogenic material, *Ber. Polarforsch,* 1993, vol. 127, pp. 93–159.

Zakharov, V.F., *Morskie l'dy v klimaticheskoi sisteme* (Marine Ice in the Climate System), St. Petersburg: Gidrometeoizdat, 1996.

Translated by M. Bogina